THE ORIGIN OF SINUOUS RILLES

VIVIEN GORNITZ
Goddard Institute for Space Studies, New York, N.Y., U.S.A.

(Received 5 December, 1972)

Abstract. This report describes the distribution and morphology of sinuous rilles and presents data on rille geometry. Examples of the relation between sinuous rilles and the regional structure are given. Leading theories for the origin of sinuous rilles are discussed and evaluated. It is concluded that the general weight of evidence is against water erosion. The ash flow theory is not excluded, but evidence in its favor is weak. The best explanations involve lava tube formation for certain sinuous rilles, and faulting for others. In some cases, a gradation between faulting and igneous activity is noted.

1. Introduction

Sinuous rilles are enigmatic lunar features, whose origin has been widely debated. The nature of sinuous rilles assumes special interest in view of the recent Apollo 15 landing site near Hadley Rille and the discovery of similar features on the Mariner 9 TV pictures from Mars.

Sinuous rilles are winding, meandering channels or valleys in the lunar surface, unlike normal rilles that are either straight or very gently curved (large radius of curvature). The latter are generally considered to be graben-type faults. Crater chains (linear arrays of partially overlapping craters) are excluded from this definition, as are the highly irregular fractures (rilles) confined entirely within some crater floors. Sinuous rilles may occasionally grade into normal rilles or crater chains. The majority of sinuous rilles occur in the maria on the lunar nearside, at mare-highland boundaries, but a few begin in the highlands. Most are concentrated around the margins of Mare Imbrium and Oceanus Procellarum. Somewhat over half of the observed rilles appear to originate in craters or irregular depressions; about a fifth taper – becoming narrower and shallower with increasing distance from their presumed source. Sinuous rilles can be over 200 km long and 4–5 km wide, but more typical dimensions are lengths of 30 to 40 km and widths of less than one km.

Various theories have been advanced for the origin of sinuous rilles, but none has been entirely satisfactory. Some scientists have proposed that the rilles represent water-eroded streams, or valleys carved by ice-melted water under a rubble-covered permafrost (Peale *et al.*, 1968; Burke *et al.*, 1970). The basic argument in favor of water erosion lies in the alleged morphological similarity between sinuous rilles on the Moon and terrestrial rivers, particularly with respect to meandering oxbow bends or goosenecks. However, evidence to be presented below will show that lunar rille geometry differs considerably from terrestrial rivers.

Other theories introduce different fluids – namely the ash gas suspension of a nuée ardente (Cameron, 1964) or molten lava forming collapsed lava tubes (Greeley, 1971). An alternative explanation postulates fluidization of gases along fractures (Schumm,

The Moon **6** (1973) 337–356.

1970; Schumm and Simons, 1969; McCall, 1970). Gases exsolved from lunar magma along faults would flow sufficiently rapidly to the surface to carry particles in suspension.

2. Classification of Sinuous Rilles With Some Examples

The classification presented here is purely descriptive, but any theory of origin must account for the observed features.

A. PLAN VIEW OF SINUOUS RILLES

(1) *Ordinary* sinuous rilles curve and wind, by definition. They often run parallel to mare-highland contacts, but manage to avoid topographic obstacles (e.g. Hadley Rille passing around the northern tip of Hadley promontory L.O. V-105M; or a rille south-west of Tobias Mayer, L.O. V-165M, which skirts the edge of a dome).Yet in some cases the rilles truncate mountains or wrinkle ridges (Rima Prinz II, L.O. V-189, 190; Marius Hills Rilles, L.O. V-213M; north of Gassendi, L.O. IV-137H), ignoring the topographic gradient. Over half the sinuous rilles begin in depressions, but the rest have no obvious source and just fade away at either end (e.g. Rima Sharp I. L.O. IV-158H).

(2) *Gooseneck*. This type of rille has very tight meanders that resemble the oxbow bends or goosenecks of mature rivers. Examples include the inner rille of Schroeter's Valley (L.O. V-204H) and rilles on the Aristarchus Plateau (L.O. V-209M).

(3) *Pseudocoalescence of craters*. Parallel arc segments on opposite sides of rille. Examples include Rima Plato II (in part) L.O. V-130, Prinz Rilles L.O. V-189, 190, Rima Posidonius L.O. IV-86H.

(4) *Branching*. Sinuous rilles with one or more branches include Rima Plato II, Rima Aristarchus III, L.O. IV-151H, and a rille north of Gassendi in O. Procellarum L.O. IV-137H.

(5) *Angular*. The rille zigzags; bends are not anticipated by the topography. The geometry and alignment parallel to other lineaments suggest fault control. e.g. Schroeter's Valley; Rima Prinz I; Marius Hills rilles; Rima Conon L.O. IV-102 H.

(6) *Rille within a rille*. Some wide-floored rilles have inner rilles that are more serpentine than the outer one. e.g. Schroeter's Valley; Alpine Valley L.O. V-102; Rima Prinz I L.O. V-188; Rille on west rim of Plato L.O. IV-127 H.

B. CROSS-SECTIONS OF SINUOUS RILLES

(1) V-shaped – common. e.g. Hadley Rille L.O. IV-102H, V-105M
(2) U-shaped – also common. Rima Bode I L.O. IV-109 H
(3) Flat-bottomed. These often contain inner rilles.
Examples: Prinz Rilles, Schroeter's Valley, Alpine Valley.

3. Geometry of Sinuous Rilles

The width, depth and slopes of several prominent rilles having high resolution photo-

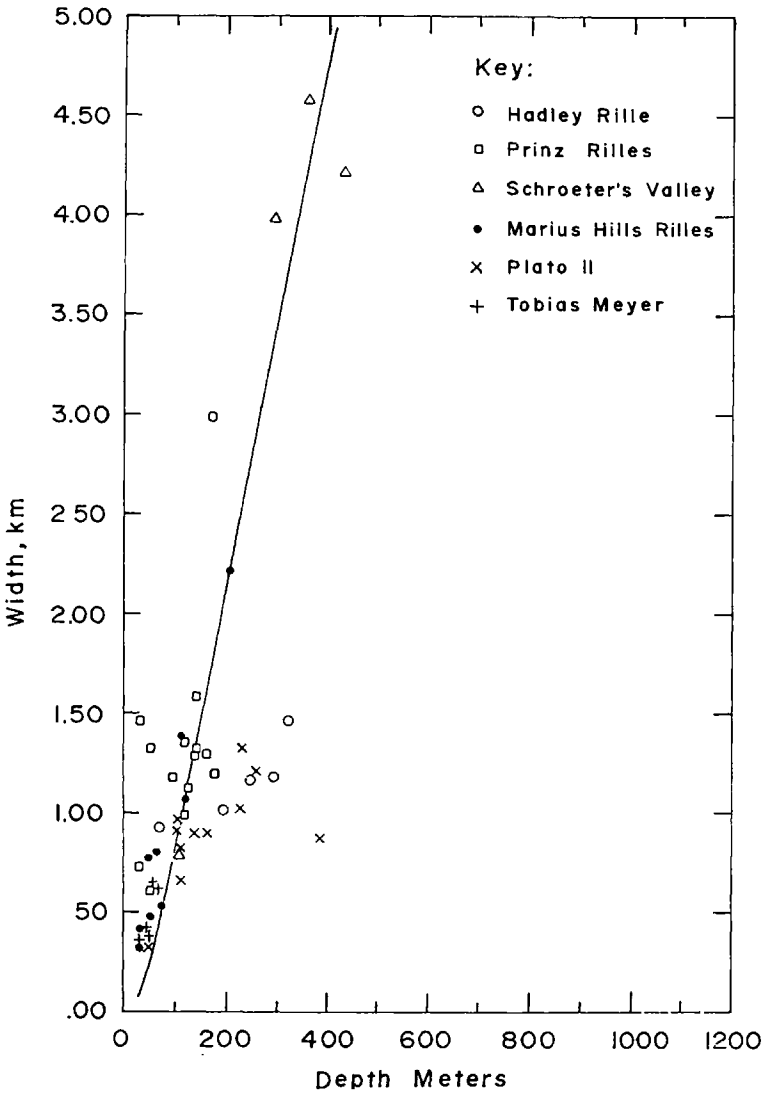

Fig. 1. Relation between width and depth of sinuous rilles.

coverage* were measured, from the shadow length and knowledge of the sun angle (angle of illumination). The relation between width and depth is roughly linear (Figure 1). There is a slight tendency for this ratio to increase downstream. Slope angles of rille walls range between 10° and 23°, with an average of 17°.

The gradients of several rilles were estimated from U.S. Army Topographic Command Maps at 1:250000 scale.** For instance, the Prinz I Rille has a gradient of 0.0224 or 1°17′, from its source crater to the sharp bend; and 0.0026 or 0°9′ from the bend to its end. The gradient of Prinz II is 0.0063 or 0°21′. By comparison, lower stretches of rivers on their floodplains may be even less than that: the Arkansas

* Prinz I, II, Prinz with rectangular crater, Schroeter's Valley, Marius Hills I, II, Hadley, Tobias Mayer P.

** More accurate statements on the gradients and width/depth relations will be possible only when the detailed topographic maps prepared from high resolution Apollo 15 photography become available.

River in its last 300 miles has a gradient of only 0.00018 (Gilluly, 1968). Gradients of terrestrial lava tubes may also by quite low; e.g. 0°28′ for some tubes in Bend, Ore. (Greeley, 1971b) and 0°35′ for the Bandera Tube, and 0°45′ for the Twin Craters Tube in New Mexico (Hatheway and Herring, 1970).

Longitudinal bottom profiles (elevations at the bottom of the rille plotted against source distance) were prepared for the Prinz rilles, Hadley and Marius Hills rilles.

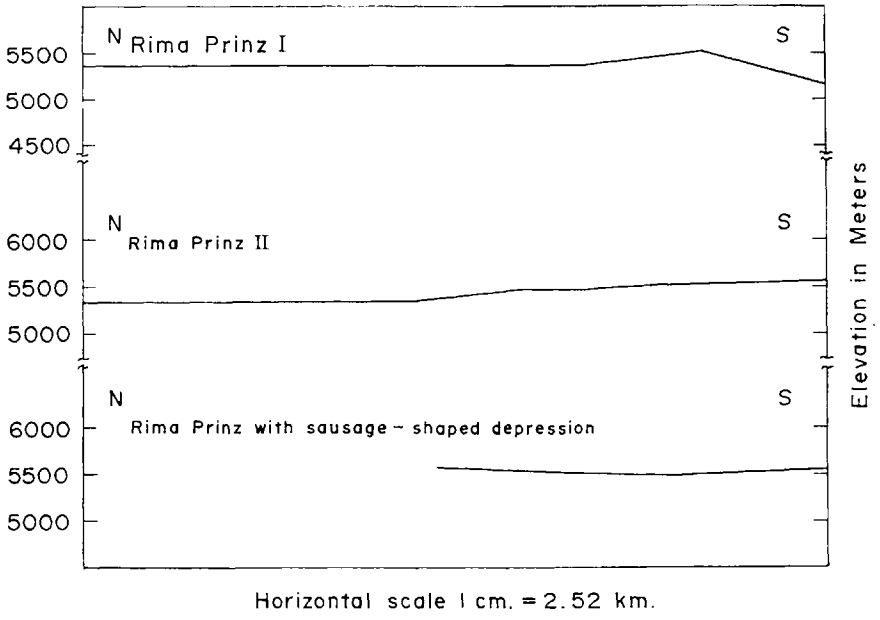

Fig. 2a. Longitudinal bottom profiles of the Prinz Rilles.

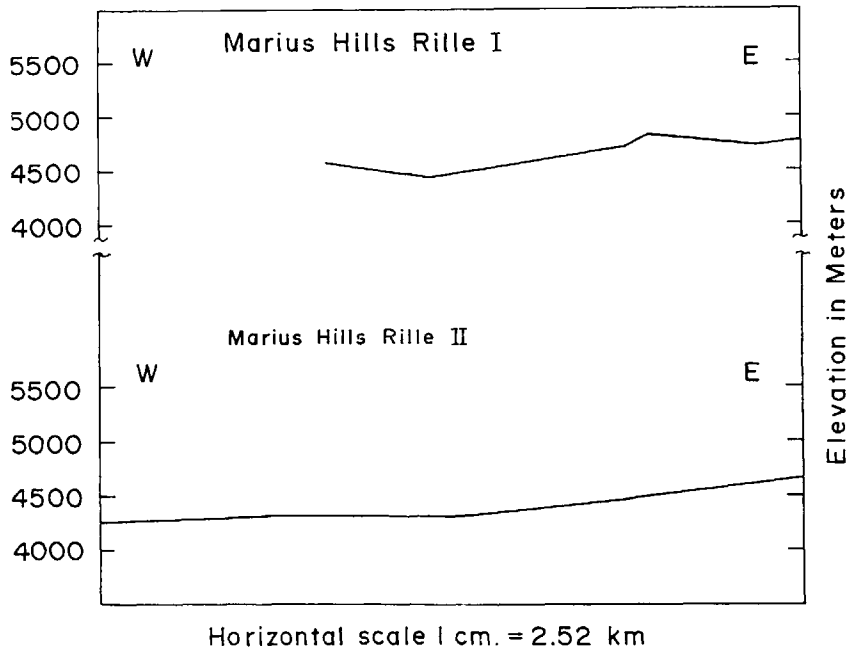

Fig. 2b. Longitudinal bottom profiles of the Marius Hills Rilles.

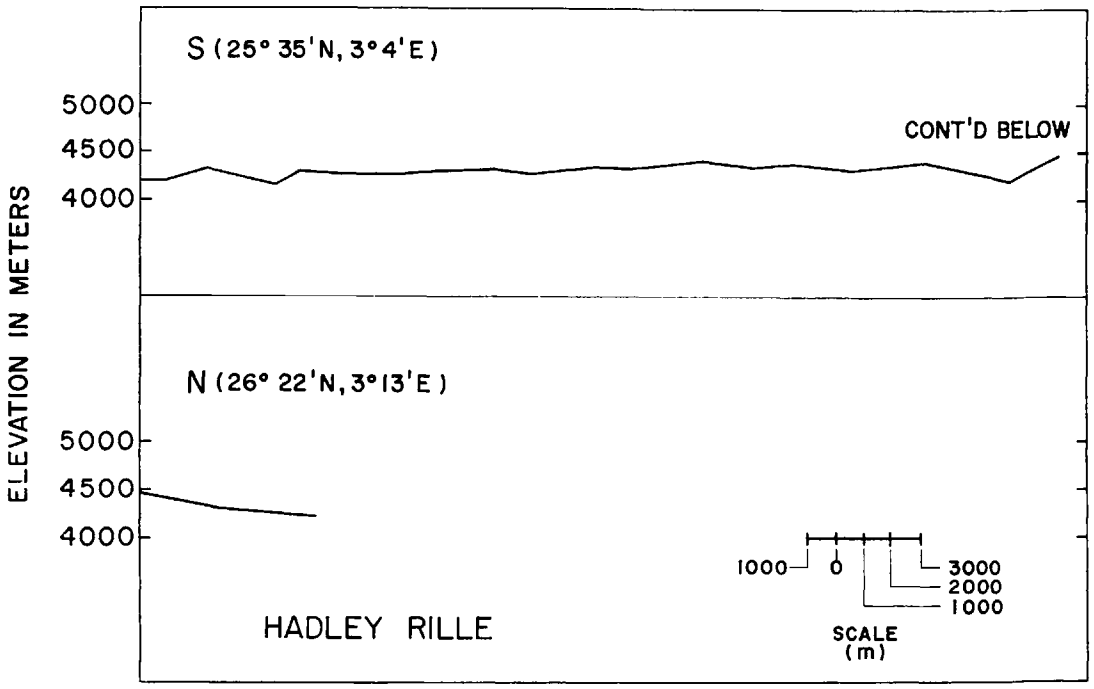

Fig. 2c. Longitudinal bottom profile of Hadley Rille.

Prinz I and II, Marius Hills I (northern) and II (southern) generally slope downhill (Marius Hills II gradient is about 0.0132 or 0°45′). However the bottom of the source crater of Prinz I rille is deeper than its termination (Figure 2a). The profile of Marius Hills rille I displays a hump where it traverses a wrinkle ridge (Figure 2b). Hadley Rille begins at a lower elevation than its termination and the depth varies irregularly along its length (Figure 2c). The foregoing illustrates that sinuous rilles while often inclined downslope, do present irregularities difficult to explain exclusively by fluid flow.

Sinuous rilles superficially resemble terrestrial rivers. Therefore, they can be compared with terrestrial rivers in regard to their morphology (Leopold *et al.*, 1964). Parameters useful in characterizing river meanders are:

(1) Sinuosity index;
(2) Meander length;
(3) Channel width;
(4) Radius of curvature.

The sinuosity index indicates the tightness of bends. Sinuosity is defined as the ratio of the channel length measured along the middle of the rille to the 'meander length' or wavelength – the distance from bend to bend in the downstream direction. Meanders termed 'sinuous' on Earth arbitrarily have ratios above 1.5. For most meandering rivers, the value of this ratio ranges between 1.3 and 4 (Leopold and Langbein, 1966). An average value of 12 measured meanders on various rivers comes to 1.63 (Table I). But most meanders on lunar rilles fall below 1.5 with an average of 1.31 (Table I).

TABLE I

Geometry of lunar sinuous rilles

Rille		Sinuosity index	Meander length	Channel width	Radius of curvature	Ratio $\frac{\text{radius of curvature}}{\text{channel width}}$
Prinz I	(1)	1.10	2.24 km	1.30 km	0.75 km	0.57
	(2)	1.26	2.27	1.36	0.62	0.45
	(3)	1.19	1.64	1.20	0.59	0.49
	(4)	2.12	1.91	0.92	0.36	0.39
	(5)	1.28	1.78	0.85	0.39	0.46
Prinz II		1.19				
	(1)	(several meanders)	1.55	1.54	0.75	0.48
	(2)	(several meanders)	2.74	1.90	0.81	0.42
	(3)	(several meanders)	2.56	1.85	0.62	0.33
	(4)	1.18	1.62	1.36	0.78	0.57
	(5)	1.04	1.78	1.56	(low bend)	–
	(6)	1.25	1.86	1.36	0.53	0.39
Prinz Rille with rectangular depression						
	(1)	1.15	2.58	1.33	0.52	0.39
	(2)	1.10	1.33	1.21	0.55	0.45
	(3)	1.13	1.52	1.17	0.45	0.39
	(4)	1.09	1.88	0.94	0.45	0.48
	(5)	1.17	2.46	0.95	0.71	0.74
	(6)	1.12	3.34	0.76	0.58	0.76
Hadley Rille						
	(1)	1.43	3.67	1.19	0.76	0.64
	(2)	1.11	1.95	0.82	0.47	0.57
	(3)	1.10	2.37	0.53	0.53	1.00
Rille near Tobias Mayer P						
	(1)	1.17	2.05 km	0.59 km	0.38 km	0.65
	(2)	1.17	2.58	0.44	0.64	1.5
	(3)	1.16	1.70	0.30	0.48	1.6
Rille on Aristarchus Plateau (V-209)						
	(1)	1.41	1.56	0.37	0.45	0.12
	(2)	1.78	1.23	0.42	0.39	0.92
	(3)	1.53	1.23	0.45	0.29	0.64
	(4)	1.95	1.50	0.47	0.27	0.57
Plato Rille II						
	(1)	1.23 (includes several meanders)		0.98	0.70	0.71
	(2)	1.69	6.23	0.98	0.77	0.79
	(3)	1.40	6.21	1.09	1.15	1.05
	(4)	1.49	6.79	1.09	0.91	0.83

Plots of meander length vs channel width and meander length vs radius of curvature for terrestrial rivers are nearly linear exponential curves (Leopold *et al.*, 1964). Generally, meander lengths are 7 to 10 times the channel width. However, for sinuous rilles, the meander length is not much more than twice the channel width. Typically for terrestrial rivers, the ratio between radius of curvature and width falls between 2 and 3, with 66% lying between 1.5 and 4.3. The average value of this ratio found for lunar rilles, on the other hand, is usually less than 1; mean value = 0.68 (Figures 3–4, Table II). No correlation was found between meander length, channel width and radius of curvature. The results contrast strongly with terrestrial rivers. Among the lunar sinuous rilles measured, the channel is wide relative to the meander length and radius of curvature is very small. Lunar rilles in stretches approach the hypothetical case of overlapping semicircles offset by one radius. If the rilles were formed by a fluid, this had erosive characteristics quite different from water.

The geometry of several lava tubes lies in between that of terrestrial rivers and lunar rilles. Like rivers, the meander length of lava tube is many times the channel

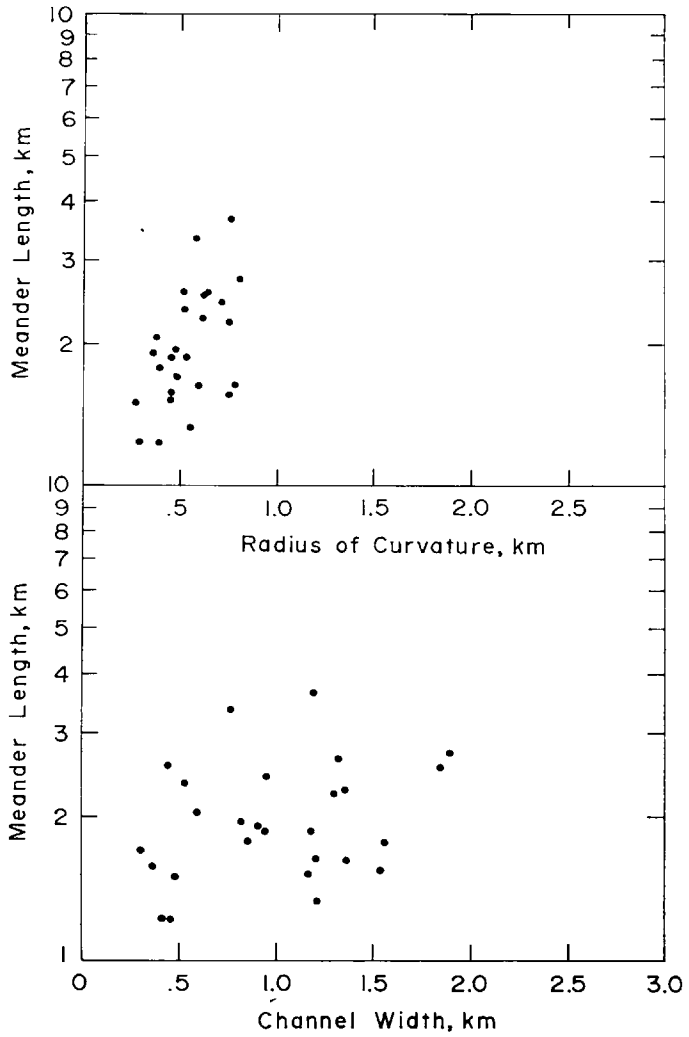

Fig. 3. Geometry of sinuous rilles.

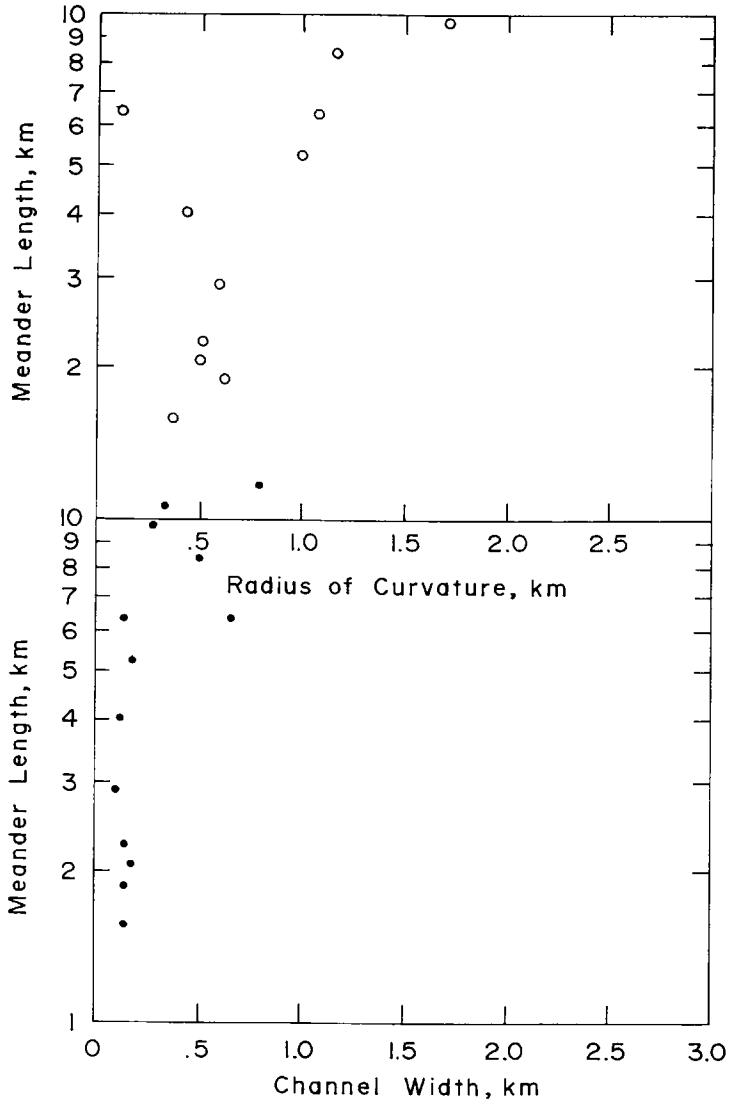

Fig. 4. Geometry of terrestrial rivers.

width, and the ratio of the radius of curvature to the channel width is close to 2. The sinuosity is lower than for rivers, with an average value of 1.3 among 14 tubes measured.

Lava channels or tubes develop along the most rapidly moving part of the lava flow. Channels frequently wind, since the low slope and rapid flow promote meandering. The tubes, on the other hand, are usually discontinuous segments exposed by collapse. The width and depth vary irregularly along the length, and branching is common.

4. Structural Control of Sinuous Rilles

If the course of sinuous rilles appears influenced by the regional structure, e.g. if segments of the rille show alignment parallel to prevailing fault, fracture on lineament directions, then the structure is said to 'control' the path of the rille. A similar situation occurs commonly in terrestrial drainage basins, where joint or fracture lineaments

TABLE II

Geometry of river meanders

River; Site	Sinuosity index	Meander length	Channel width (av.)	Radius of curvature	Ratio $\left\{\frac{\text{radius of curvature}}{\text{channel width}}\right.$
Arkansas River; Pastoria Quad., Ark.	2.36	6.35 km	0.655 km	1.10 (av)	1.68
White River; Aberdeen Quad., Ark.	1.98	2.07	0.162	0.498	3.07
Mississippi River; Big Island Quad., Ark.-Miss.	1.32	11.8	0.782	2.06	2.64
White River; Crocketts Bluff Quad., Ark.	2.07	1.89	0.143	0.614	4.29
White River; Crocketts Bluff Quad., Ark.	1.28	2.26	0.145	0.505	3.48
White River; Crocketts Bluff Quad., Ark.	1.70	1.57	0.143	0.362	2.53
Missouri River; Atchison East Quad., Mo.-Kansas	1.40	10.9	0.286	2.54	8.88?
Osage River; Bagnelle Quad., Missouri	1.72	6.35	0.132	1.07	8.05
Missouri River; Halls Quad., Mo.-Kansas	1.55	9.75	0.270	1.72	6.36
Ohio River; Maysville West Quad., Ky.-Ohio	1.10	8.4	0.503	1.16	2.32
Kentucky River; Tyrone Quad., Ky.	1.32	4.03	0.105	0.428	4.16
Kentucky River; Tyrone Quad., Ky.	1.76	2.9	0.095	0.595	6.25
Colorado River, Austin West Travis Co., Texas	1.71	5.28	0.168	0.97	5.76
	average 1.63				average 4.57

become accentuated by erosion, since they represent zones of weakness in the country rocks.

On the Moon, Hadley Rille, the Prinz Rilles and Schroeter's Valley illustrate the effect of structural control, to varying degrees.

Hadley Rille, landing site of Apollo 15, is located at the foot of the northern part of the Apennine Mountains (26° N, 3.5° E)), close to the Apennine Scarp – the eastern boundary of Mare Imbrium. The lunar canyon is about 1 to 1½ km wide, 300 m deep and 130 km long. It begins in a narrow, elongated V-shaped cleft, runs parallel to the base of the Apennine Scarp, then veers abruptly to the northwest, fades away beyond the promotory west of Mt. Hadley, but reappears and merges with the Fresnel

Rille system (Figure 5). The canyon is V to U-shaped in sections with an average slope of about 21°.

Cross-sections show that parts of Hadley Rille lie on the crest of a shallow rise (Figure 6). The east side of the rille near the Apollo 15 landing site stands an estimated 40 m higher than the west side. Topographic low points are situated to the west of Hadley C Crater. The ridge at the crest of the rille may have resulted from arching or structural uplift as suggested by the gentle outward dips in the underlying rocks

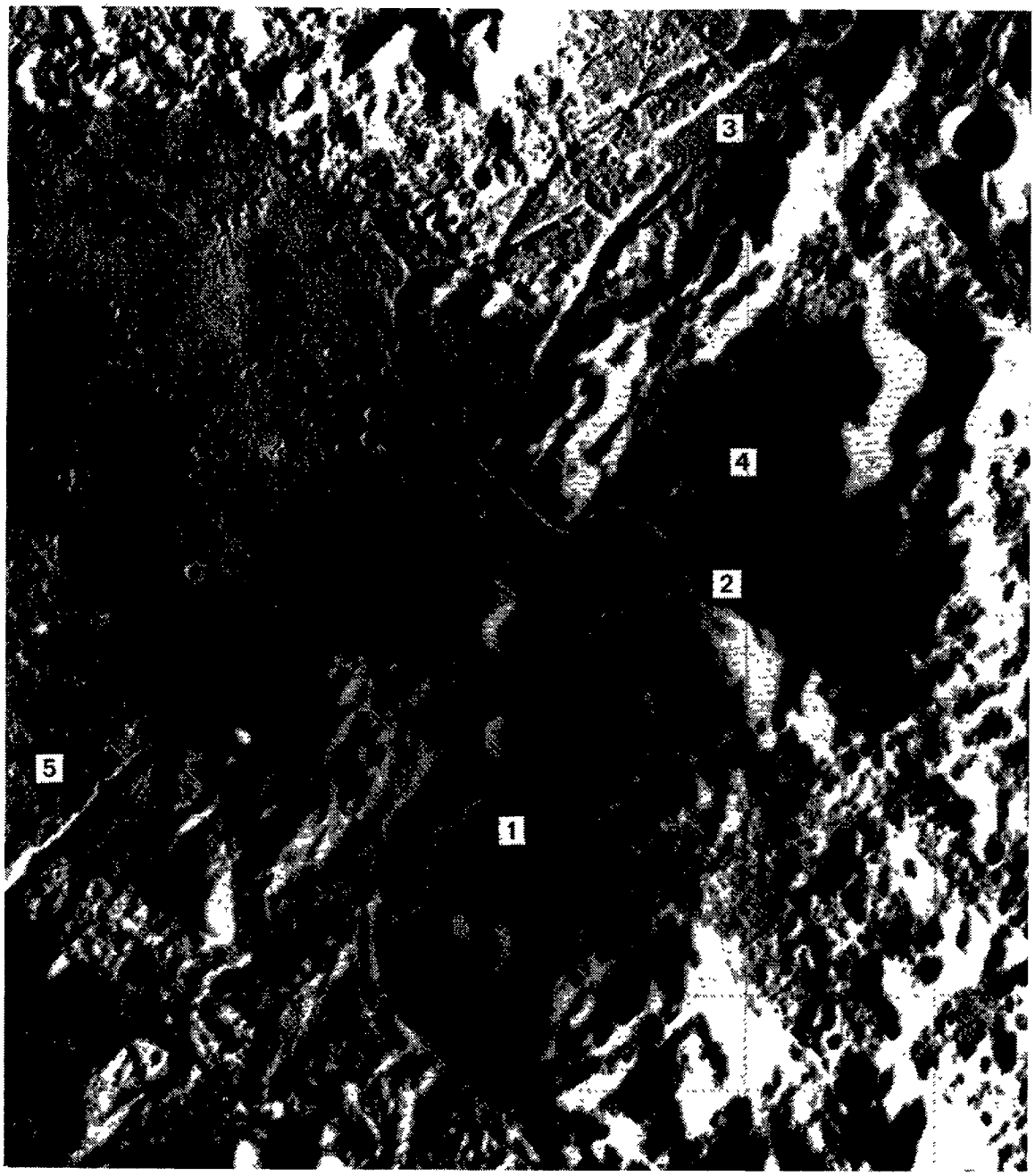

Fig. 5. Hadley Rille and the Apennine Front (Apollo 15 photograph). (1) Apennine Scarp; (2) Apennine Front; (3) Fresnel Rilles; (5) Bradley Rille; (4) Mt Hadley.

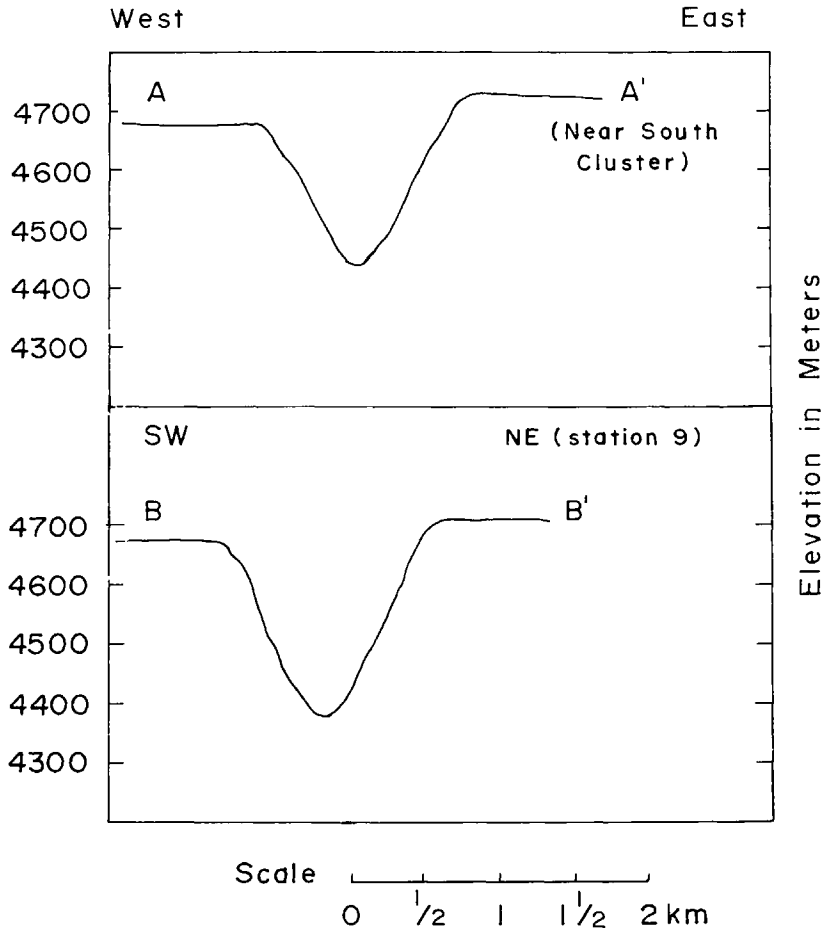

Fig. 6. Cross-sections of Hadley Rille (topographic data from *Science*, January 28, 1972).

(Prelim. Rept. on Geology of Apollo 15 site, August 1971). Greeley (1971a) on the other hand, infers that lava traveling down the rille had overflowed its banks repeatedly, building up a levee, much like a river.

Photographs taken by the Apollo 15 astronauts show horizontal outcrops of multilayered basalt (confirmed by returned lunar samples) along the upper walls of the rille. The layering is universally attributed to superposition of a sequence of lava flows. While examples are known of two or three successive lava flows confined to the same channel, it seems unusual that lava could erode such a deep gorge. Many lava tubes are approximately cylindrical in cross-section and therefore the width to depth ratio should be roughly two (the ratio may increase because of mass-wasting, slumping, etc. along the walls; irregular and key-hole shaped tubes also exist). The width-depth ratio for Hadley Rille is about 4:1, but is still larger for other sinuous rilles. Furthermore, the canyon does not go downhill. A bottom profile (prepared from the 1:250000 topographic map and from Apollo 15 photometry) shows that the rille begins at a lower elevation than its termination (Figure 2c). The depth varies irregularly along its length. While some variation may be caused by infilling or slumping of material from the rille walls, the increased elevation at the northern end implies

that tectonic displacements have occurred. The latter view is supported by the close correlation between the course of Hadley Rille and the regional structure (Figure 5).

Sudden bends in the course of Hadley Rille follow the prevailing fracture pattern rather than regional topography. In the Hadley-Apennine region, NE-SW and NW-SE fracture systems predominate. These stem from readjustments in the lunar crust, after excavation of the Imbrium basin by the explosive impact of a large asteroid.

The NE-SW trending fracture system (av. N46.3°E) in this area is concentric with the edge of the Imbrium basin and includes rilles such as Rima Bradley, a fault along the 'peninsula' west of Hadley Rille, and the Fresnel Rilles. Circular mare basins commonly are bounded by concentric arcuate rilles (e.g. M. Humorum and M. Nectaris). Hadley Rille, measured in the nearest straight line from its source depression to the bend at the Apennine Front runs N42°E, roughly parallel to the base of the Apennine Scarp. This cliff is probably a fault along which material had been down-dropped toward the mare basin, and rectangular blocks of pre-Imbrium rocks had been uplifted subsequent to the Imbrium event.

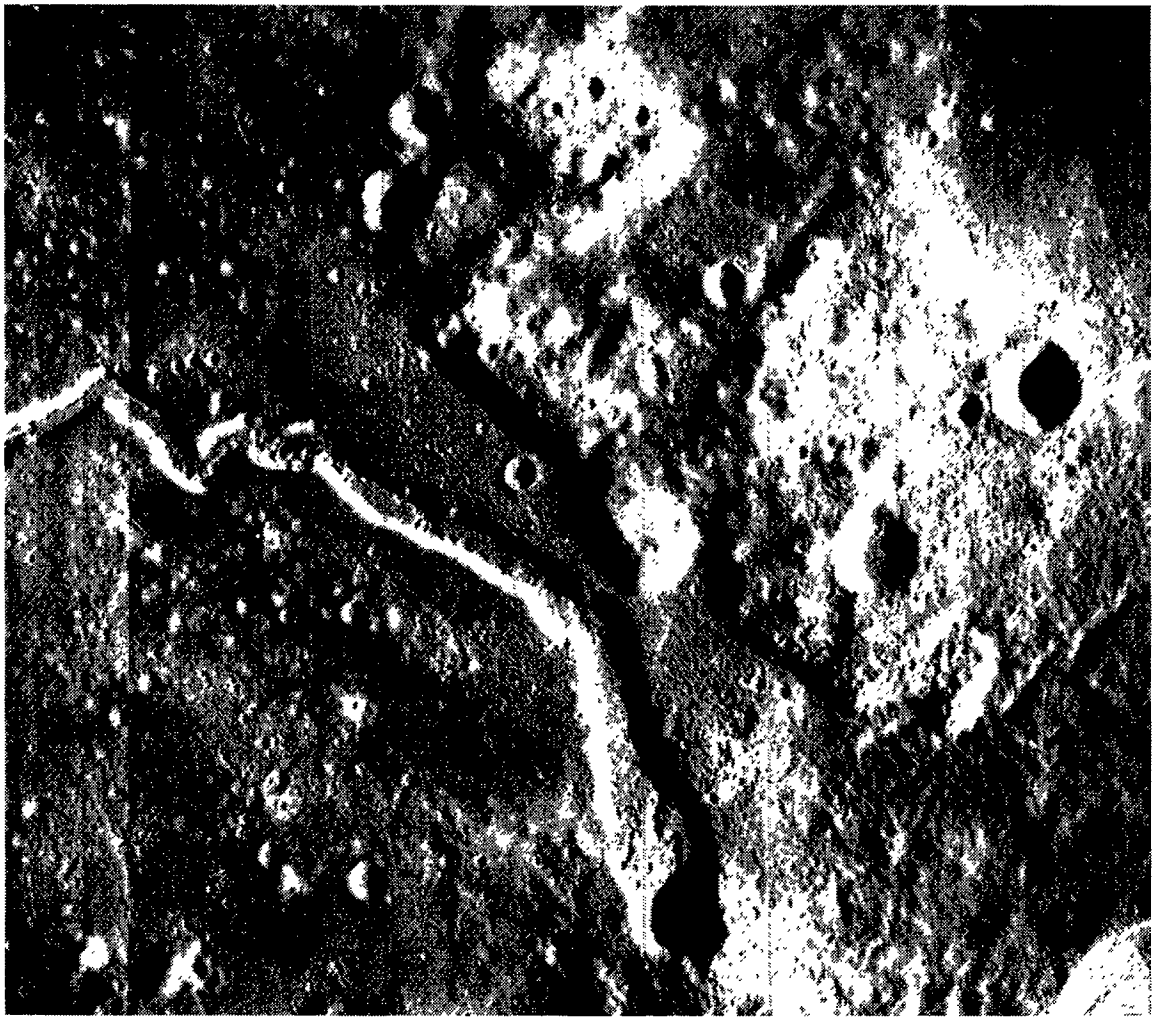

Fig. 7. Schroeter's Valley and the Cobra Head (Lunar Orbiter V-204 M).

Another rille system, radial to the center of Mare Imbrium, includes the Alpine Valley, rilles near Ptolomeus, Alphonsus and in Fra Mauro. In the Apennine-Hadley area this system trends in a N45°W direction, such as marked by the Apennine Front, the base of Mount Hadley and the Archimedes Rilles. The abrupt turn of Hadley Rille to the NW at the foot of Hadley and the nearly right-angle turn it makes around the promotory west of Mt. Hadley illustrate the effect of the NW-fracture pattern on the course of the rille.

Hadley Rille ultimately intersects the Fresnel Rille system, suggesting a relationship between sinuous and straight rilles. Hadley Rille may have originated as an irregular fracture in the mare, perhaps opened by the shrinkage of lava as it cooled and outgassed. The kinks and turns were controlled by the dominant fracture systems established during the Imbrium impact. Sinuous rilles, like arcuate rilles, frequently

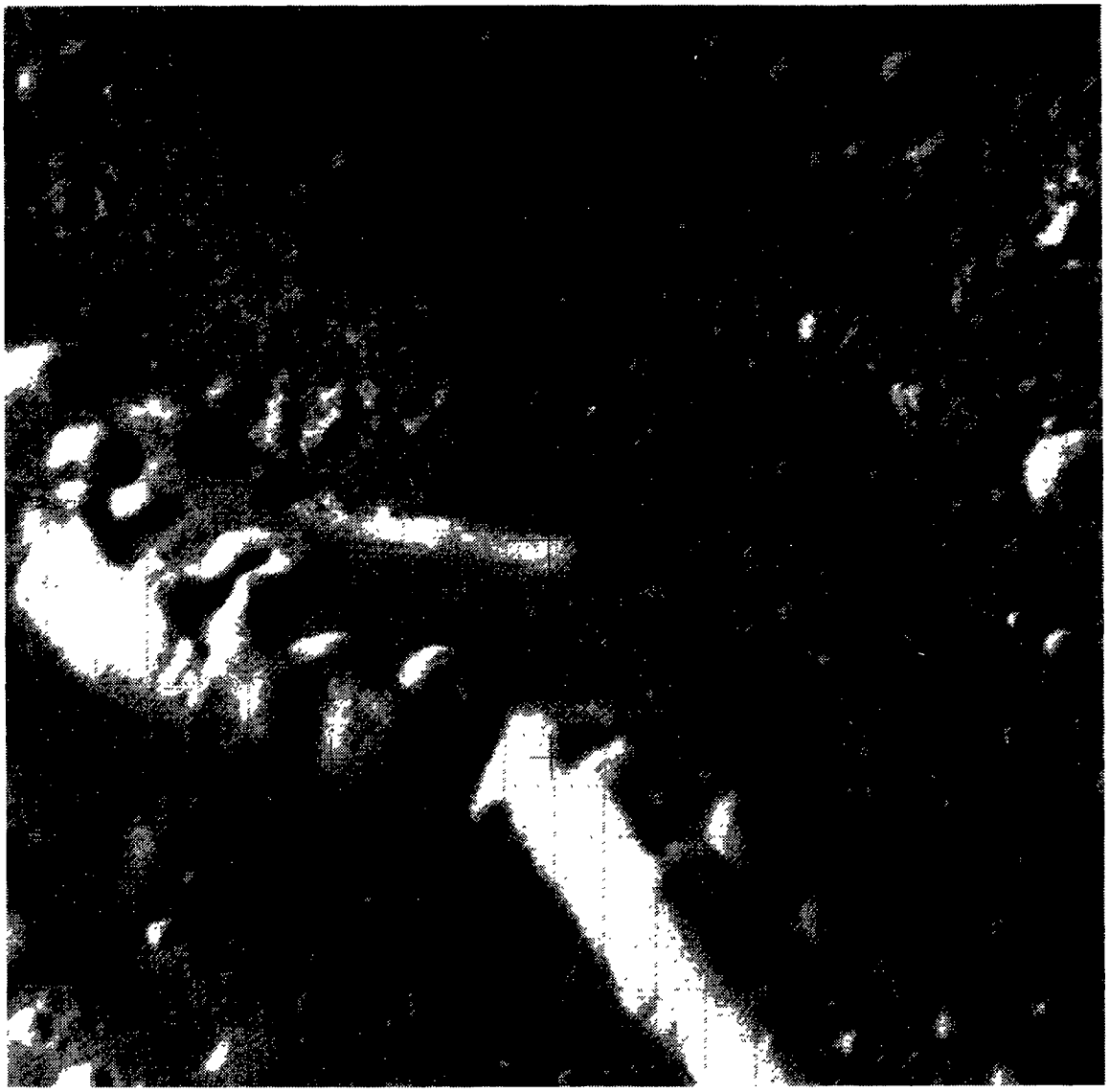

Fig. 8. Inner sinuous rille of Schroeter's Valley (Apollo 15 photograph No. 15-2969).

occur near mare-highland boundaries and may mark sites of structural weakness in the lunar crust.

Schroeter's Valley, 170 km long, as wide as 4.5 km and as deep as 404 m, forms the largest sinuous rille on the Moon (Figure 7). Actually, the rille is fairly angular and its segments parallel the regional fracture trends of ~N45°E and N40°W, resulting from block faulting, possibly related to the 'lunar grid' system. The Aristarchus Plateau (very low in albedo) displays a complex volcanic history, comprising ash and lava flows, maar craters, calderas and domes (see Aristarchus and Seleucus quadrangle maps I-465 and I-527).

A very sinuous rille meanders along the length of its flatbottomed floor. Schumm (1970) claims that parts of the inner rille consist of semi-circular craters, formed by venting of gases along a fault at the base of the Valley's wall. In experiments to simulate the geometry of 'coalesced craters' Schumm released compressed air through a series of vents in a sand-filled flume producing rille-like structures. However, photographic examination of the inner rille shows that it is continuous, forms oxbow meanders (or 'goosenecks') and wanders from one side of the valley to another, as a river confined to its floodplain (Figure 8). Whereas Schroeter's Valley appears to be a fault-controlled graben or rift valley, the inner rille cannot be explained by the same process. Instead, it seems to have been carved by a fluid – perhaps a lava (or ash) flow emanating from the depression at the Cobra Head. Studies of terrestrial lava

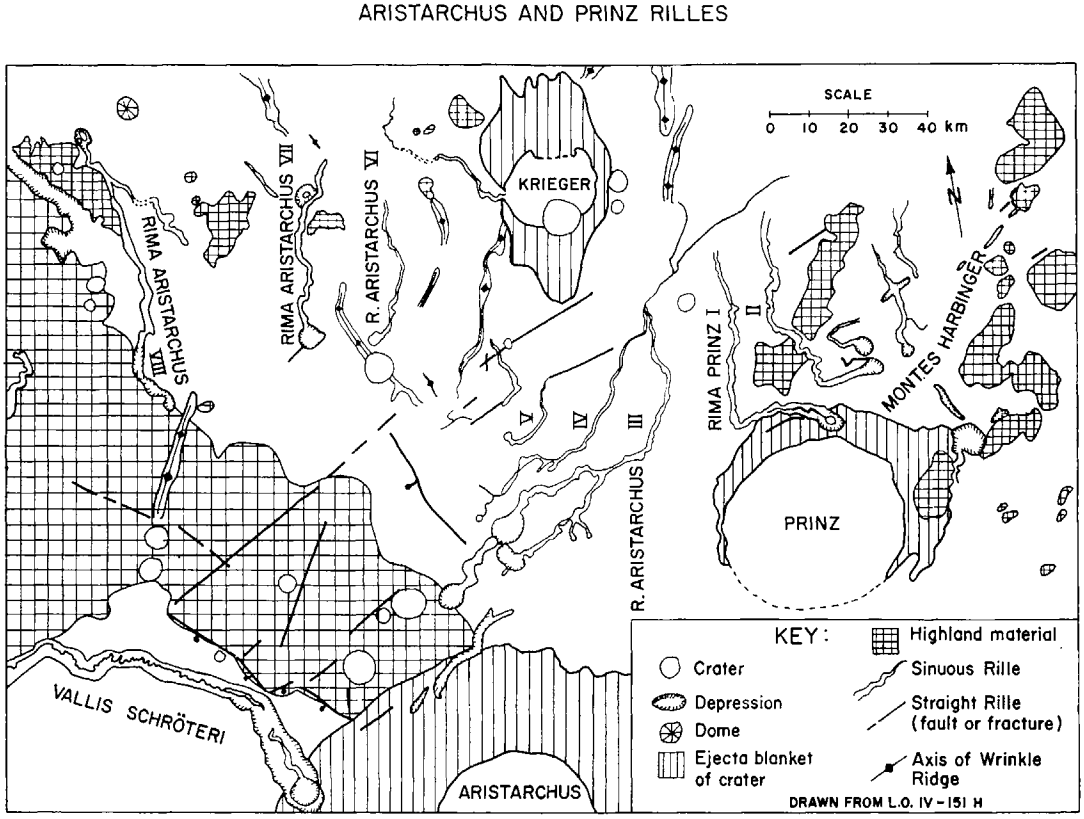

Fig. 9. Prinz and Aristarchus Rilles – geological sketch map (drawn from L.O. IV-151 H).

flows in several areas, particularly in smooth (pahoehoe) basalt indicate that lava flows frequently advance by means of winding tubes and open channels (Greeley, 1971b, c).

Structure governs the course of the Prinz Rilles, north of Aristarchus in O. Procellarum, to a lesser degree than at Hadley Rille or Schroeter's Valley. While the Prinz (and Aristarchus) rilles usually start in shallow craters and generally follow the topographic gradient northward, some segments trend ~N73°E, parallel to a local fault direction. This lineation affects the initial portions of Prinz Rilles I and II before they turn north, a sausage-shaped crater traversed by yet another rille, and some segments of Aristarchus Rilles III, IV, V and Va (Figure 9). A NNW fracture trend may also have enabled Rima Prinz II to cut across the mountain. However, the very sinuous character of the rilles, their origin in depressions and general downslope gradient suggest the action of fluid erosion.

5. Discussion and Conclusions

The origin of sinuous rilles has aroused lively scientific debate, but no consensus has been reached as their mode of formation.

A. FLOWING WATER

Some scientists have suggested that the rilles were carved by flowing water, or by ice-melted water beneath a rubble-covered permafrost (Peale *et al.*, 1968; Burke *et al.*, 1970). However, water would not be retained on the lunar surface for sufficient lengths of time to carve out river valleys, due to the near-vacuum conditions. The Apollo 14 active seismic experiment rules out the presence of an extensive permafrost layer (Watkins and Kovach, 1972). Furthermore, analysis of the various Apollo lunar samples has demonstrated the extreme deficiency of volatile elements, especially water, in the moon rocks (Morrison *et al.*, 1970; Keays *et al.*, 1970; *Science*, Jan. 1970). Hydrous minerals were nearly totally absent*. The evidence indicates that the loss of volatile elements occurred at the very earliest stages of lunar history. On the other hand, sinuous rilles represent relatively young features, having been superimposed upon the maria. Furthermore, upon careful examination, even the morphological argument breaks down. This study has shown that the geometry of terrestrial rivers (the relation between meander length, channel width and radius of curvature) differs considerably from lunar sinuous rilles.

Theories of fluid erosion require that sinuous rilles display a downhill gradient, a condition often but not always met. Nor do they account for sinuous rilles cutting across topographic obstacles such as wrinkle ridges, as in Oceanus Procellarum, or mountains (Prinz II in the Harbingers), or even changing direction abruptly for no apparent reason.

* Reports of individual grains of amphibole and goethite were presented at the 1972 3rd Lunar Science Conference in Houston.

B. ASH FLOW EROSION

Another means of fluid erosion may be achieved by the ash-gas suspension of a nuée ardente (Cameron, 1964) or fluidization of gases along fractures (Schumm, 1970). The ash flow theory notes the frequent fracture control of sinuous rilles and their gradation from normal to sinuous (e.g., the Diamondback Rille in the Maskelyne Rille System; Blodget and Lowman, 1970). It also accounts for the 'coalesced' craters of some rille segments and crater chains like Davy Rille or Hyginus Rille.

However, evidence for former extensive gaseous activity is weakened by the lack of volatile elements in the lunar rocks. Gaseous emissions along a fracture should produce 'coalescing' or overlapping craters, whereas sinuous rilles show continuous meanders which have parallel arc segments on opposite sides of the rille (see Figure 8)

Nuée ardentes or ash flows do not gouge out channels resembling sinuous rilles. Mostly, ash flows follow preexisting valleys. Moreover, extensive ash flows on the moon would not be anticipated because explosive igneous activity, governed to a large extent by the sudden release of gases, is usually associated with more silicious rocks like andesite or rhyolite. They possess a higher viscosity than basalt, which would impede the escape of enclosed gases, leading to violent eruptions (Rittmann, 1962). However, the bulk of returned lunar material and remote sensing experiments (e.g. X-ray fluorescence or gamma-ray spectrometers) show that the Moon's surface is largely composed of basaltic rocks.

C. LAVA TUBES

The theory that sinuous rilles form by the collapse of lava tubes (Greeley, 1971) has gained support, since the Apollo missions found basaltic rocks in the maria.

Terrestrial lava tubes and channels up to 28 km long and 30 m wide have been extensively mapped (Hatheway and Herring, 1970; Greeley, 1971). These studies have determined that smooth pahoehoe basaltic lava (low viscosity) frequently advances by means of meandering tunnels or open channels. Tubes may even be stacked one over the other (Greeley, 1971b). The gradient needed for lava tube formation is rather low – about 0°30′. The serpentine nature of certain lunar rilles and their origin in depressions can best be explained by fluid erosion. Since water has been effectively ruled out for reasons discussed above, lava flows could present a possible alternative. The Apollo missions have established that the maria are covered by vast sheets of basaltic lava, thus emphasizing the wide extent of lunar volcanism. One persuasive example of a lunar leveed lava channel, which ends in a flow downslope may be found on the SW outer flank of Aristarchus (Figure 10).

Laboratory experiments with synthetic lunar rocks of Apollo 11 composition show that the viscosities of lunar basalts at 1400 °C is about $\frac{1}{10}$ that of terrestrial basalts (Murase and McBirney, 1970). Assuming the same flow thickness and slope angle, lunar lava could travel 1.9 times farther than on earth before congealing. Furthermore, the thermal conductivity of lunar rock is $\frac{1}{2}$ that of molten terrestrial basalt. Because of the reduced thermal conductivity, a rapidly-cooled surface crust could act as an

Fig. 10. Leveed lava channel on the SW outer rim of Aristarchus (L.O. V-197 H_3).

efficient insulator, permitting flows to continue over long distances, If other factors remain constant, the reduced lunar gravity could support a larger width roof. The net result is that the scale of collapsed lava tubes or channels on the Moon could be several times larger than on Earth.

However, unless the mechanics of lava tube formation on the moon involve factors

unlike any on Earth, it is still difficult to understand how flowing lava could produce a canyon, such as Hadley Rille that is 10 times deeper and longer than any known terrestrial lava tunnel. The explanation of this difference in scale still remains a major problem in understanding the origin of sinuous rilles.

D. FAULTING AS A CAUSE OF SOME SINUOUS RILLES

The foregoing discussion demonstrates that no single explanation can account for all aspects of sinuous rilles. Segments of sinuous rilles are often aligned parallel to regional lineaments. Some rilles cut across topographic high points and do not show a downhill gradient. Sinuous rilles may occasionally transform into straight rilles. They also occur frequently parallel to mare-highland edges, which are often fault controlled.

Fig. 11. Rilles, crater chains and ridges, eastern Mare Fecunditatis south of Secchi U (Apollo 11 photograph AS 11-42-6309).

These observations suggest that sinuous rilles are internally produced features, in some cases resulting from highly irregular fractures or faults, and in others, due to various magnifestations of igneous activity, particularly lava channels or collapsed lava tubes.

Normal straight to angular rilles, generally independent of topographic gradient, and following the regional fracture pattern, occasionally grade into crater chains or sinuous rilles (e.g. stretches of the inner rille of the Alpine Valley, the mare termination of Rima Plato II, rilles in the Triesnecker area). The straight to arcuate rilles constitute grabens (or rift valleys bounded by inward-dipping normal fault planes, Baldwin (1963), Quaide (1965), and McGill (1970)). Crater chains such as Davy Rille, Hyginus Rille and one on the floor of Mendeleev crater, could indeed represent the alignment of maars (gas explosion vents) along fractures as outlined by Schumm (1970).

An Apollo 11 photograph taken south of Secchi U on the eastern edge of Mare Fecunditatis (0.5° N, 42° E) illustrates clearly the connection between diverse features, including crater chains. (Figure 11) A somewhat sinuous rille emerges from a rimless, dark-haloed crater, branches, becomes angular and cuts across a ridge. The ridge, in turn, covers part of a straight rille. Lava flows from the base of the ridge may have filled the southern part of the rille which is much shallower than the northern end. An angular crater chain composed of coalesced craters (not meanders) commences at a nearby irregular crater. Subsidence craters, straight rilles (faults), gas explosion vents, and ridges (probably volcanic domes) all intersect in a complex manner involving a combination of structural and igneous processes.

Similarly, many sinuous rilles may owe their origin to an interaction of the various processes outlined above. Many of the smaller sinuous rilles that begin in craters, show a downhill gradient, and whose meanders are very tight, may have originated as lava channels or collapsed lava tubes. Others may simply form by irregular faulting, perhaps locally including gas venting. The frequent association of sinuous rilles with mare-highland boundaries may be significant from a structural point of view, although a few rilles (e.g. near Plato) begin in the highlands.

Acknowledgements

The writer expresses appreciation to Dr R. Jastrow for helpful advice and discussions. This research was carried out at the Goddard Institute for Space Studies under a National Academy of Sciences research associateship.

References

Blodget, H. W., Lowman, P. D., Jr., and O'Keefe, J. A.: 1970, Goddard Space Flight Center X-644-70–165.

Burke, J. D., Brereton, R. G., and Muller, P. M.: 1970, *Nature* **225**, 1234–1236.

Cameron, W. S.: 1964, *J. Geophys. Res.* **69**, 2423–2430.

Gilluly, J., Waters, A. C., and Woodford, A. O.: 1968, *Principles of Geology*, 3rd ed., W. H. Freeman and Co., San Francisco, 687 pp.

Greeley, R.: 1971a, *Science* **172**, 722–725.

Greeley, R.: 1971b, State of Oregon Dept. of Geology and Mineral Resources, *Bull.* **71**, 1–47.
Greeley, R.: 1971c, *Mod. Geol.* **2**, 207–223.
Greeley, R. and Hyde, J. H.: 1971, Wash. NASA Tech. Mem. X-63, 022.
Hatheway, A. W. and Herring, A. K.: 1970, *Lunar Planet. Lab. Comm.* **8**, 229–327.
Keays *et al.*: 1970, *Science* **167**, 490–493.
Leopold, L. B. and Langbein, W. B.: 1966, *Sci. Am.* **214**, 60–69.
Leopold, L. B., Wolman, M. C., and Miller, J. P.: 1964, *Fluvial Processes in Geomorphology*, W. H. Freeman and Co., San Francisco.
McCall, G. J. H.: 1970, *Nature* **225**, 714–716.
Morrison, G. H. *et al.*: 1970, *Science* **167**, 505–507.
Murase, T. and McBirney, A. R.: 1970, *Science* **167**, 1491–1493.
Oberbeck, V. R., Quaide, W. L., and Greeley, R.: 1969, *Mod. Geol.* **1**, 75–80.
Peale, S. J., Schubert, G., and Lingenfelter, R. E.: 1968, *Nature* **220**, 1222–1225.
Schumm, S. A.: 1970, *Geol. Soc. Am. Bull.* **81**, 2539–2552.
Schumm, S. A. and Simons, D. B.: 1969, *Science* **165**, 201.
Watkins, J. S. and Kovach, R. L.: 1972, *Science* **175**, 1244–1245.